Photochemical Doping and Tuning of the Work Function and Dirac Point in Graphene Using Photoacid and Photobase Generators

*Jose Baltazar, Hossein Sojoudi, Sergio A. Paniagua, Siyuan Zhang, Richard A. Lawson, Seth R. Marder, Samuel Graham, Laren M. Tolbert, and Clifford L. Henderson**

This work demonstrates that photochemical doping of CVD-grown graphene can be easily achieved using photoacid (PAG) and photobase (PBG) generators such as triphenylsulfonium perfluoro-1-butanesufonate (TPS-Nf) and 2-nitrobenzyl *N*-cyclohexylcarbamate (NBC). The TPS-Nf ionic onium salt photoacid generator does not noticeably dope or alter the electrical properties of graphene when coated onto the graphene surface, but is very effective at inducing p-doping of graphene upon exposure of the PAG-coated graphene sample. Likewise, the neutral NBC photobase generator does not significantly affect the electrical properties of graphene when coated, but upon exposure to ultraviolet light produces a free amine, which induces n-doping of the graphene. Electrical measurements show that the doping concentration can be modulated by controlling the deep ultraviolet (DUV) light exposure dose delivered to the sample. The interaction between both dopants and graphene is also investigated. The photochemical doping process is able to tune the work function of the single-layer graphene samples used in this work from 3.4 eV to 5.3 eV. Finally, a p–n junction is fabricated and analyzed, showing that it is possible to control the position of the two current minima (two Dirac points) in the ambipolar p–n junction.

1. Introduction

Graphene, a two-dimensional sp^2 hybridized carbon lattice, has attracted significant interest due to its distinctive electrical and mechanical properties[1,2] including its high charge carrier mobility, transparency, mechanical strength and flexibility.[3] These properties have spurred research directed at modifying graphene for use in a variety of electronic, optoelectronic, and sensor technologies.[4–6] Therefore graphene may play an important role in providing an alternative to current materials (for example, indium tin oxide -ITO, or silicon) in a variety of applications, such as transparent electrodes[7,8] (which are critical elements for numerous devices such as displays, OLEDs, photovoltaic devices)[1,9] in which ground breaking performances by graphene based devices have already been shown.[10]

Tailoring the electronic properties of graphene without inducing structural defects is necessary in order to fully achieve its potential for variety of electronics applications.[4,5,11] Intentional doping of graphene (by charge or electron transfer) allows tuning of the work function of graphene without introducing large numbers of defects. A variety of doping techniques have been explored, primarily through electrostatic gating,[12] chemical interactions,[13] and intercalation.[14,15] Replacement of carbon atoms with atoms of other elements in the graphene lattice has also been shown to modulate the carrier types and concentrations in graphene to allow for p- and n-type doping; however, these methods induce structural defects in the graphene which results in a degradation in the electronic properties of doped films made using by methods.[13] Doping of graphene through charge-transfer interactions[16,17] has been shown to be an effective method to modify the electronic structure without interfering with the integrity of the sp^2 lattice.

Different types of dopants have been used, including gases,[18] metals,[8,19] polymers,[20] organic compounds and metal-organic compounds.[13,21,22] Nevertheless, most of these dopants and processes suffer from one or more of the following deficiencies: lack of scalability, failure to provide access to large dopant concentrations, limited air stability, or that they irreversibly dope the graphene upon contact, preventing modulation and tuning of doping during post-processing. Furthermore, careful control of dopant concentrations, including the ability to selectively and locally modulate doping level (e.g. via photopatterning) and thus the transport behavior from neutral to p-doped or n-doped in an area-selective manner could be very useful for a variety of applications such as circuits and sensors.[4,5,23]

J. Baltazar, Dr. R. A. Lawson, Prof. C. L. Henderson
School of Chemical and Biomolecular Engineering
Georgia Institute of Technology
Atlanta, GA 30332–0100, USA
E-mail: cliff.henderson@chbe.gatech.edu
Dr. H. Sojoudi, Prof. S. Graham
Woodruff School of Mechanical Engineering
Georgia Institute of Technology
Atlanta, GA 30332–0405, USA
Dr. S. A. Paniagua, S. Zhang, Prof. S. R. Marder, Prof. L. M. Tolbert
School of Chemistry and Biochemistry
Georgia Institute of Technology
Atlanta, GA 30332–0400, USA

DOI: 10.1002/adfm.201303796

We have previously reported several methods for doping graphene using both self-assembled monolayers (SAMs) and dip-coated films.[15,24,25] In addition, other work has shown that deposition of graphene on a substrate with pre-patterned SAMs leads to doping of graphene in a spatially controlled manner.[24] In all such cases, there was no simple method for tuning the doping level after a particular graphene device was assembled. For example, in the case of the SAM doping, the doping level is controlled by the density of SAM molecule deposition on the substrate surface when the SAM coating is made.

Photo-induced doping of graphene hence presents itself as a potentially attractive process since it would allow for facile spatial control of the doping using conventional lithography tools, opening the door to using graphene both as the semiconductor and as contacts in devices. Photochemical dopant strategies reported in the literature for graphene; however, required large exposure times and yielded very small changes in the neutrality point.[19,26–28]

The goal of the work reported here was to demonstrate a method whereby a latent dopant could be deposited in contact with the graphene film and subsequently modulated using external stimuli to tune the doping level in the graphene and also thereby its work function. Ultimately, we sought to demonstrate that such doping activation could be achieved in a pattern-wise manner. In thinking about possible methods for achieving these goals, we decided to borrow lessons from the extensive work done by our group in semiconductor lithography and photoresist technology.[29] This study has focused on developing an on-demand photochemical method for doping of graphene using photoacid (PAG) and photobase (PBG) generators. Specifically, this paper reports on examples of both PAG (triphenylsulfonium perfluoro-1-butanesufonate, TPS-Nf) and PBG (2-nitrobenzyl *N*-cyclohexylcarbamate, NBC) to easily dope graphene, and the observation that such doping can be controlled in an area-selective manner using traditional lithographic exposure tools. Electrical measurements confirm that before exposure, the graphene maintains its pristine electrical properties after being coated with the PAG and PBG compounds and that by modulating the deep ultraviolet (DUV) light exposure dose delivered to the films, the doping concentration for both the p and n-dopants can be controlled. Raman spectroscopy, X-ray photoelectron spectroscopy (XPS) and ultraviolet photoelectron spectroscopy (UPS) were used to characterize graphene samples doped using this strategy. Significantly, it is shown from UPS that this doping technique yields a work function modulation from 3.4 eV to 5.3 eV in single layer graphene. Finally, using TPS-Nf a p-n junction was fabricated and analyzed via XPS mapping and electrical measurements, demonstrating that it is possible to control the position of the two current minima (two neutrality points) in the ambipolar p-n junction with such dopants.

2. Results and Discussion

Photoacid generator (PAG) and photobase generator (PBG) compounds have been extensively studied and utilized on semiconductor microlithography. In this study, we chose TPS-Nf and NBC due to their high solubility in common solvents, ambient stability, and efficient photochemical reactivity.[30] It was anticipated that PAG compounds such as TPS-Nf could be used to p-dope graphene while PBG compounds such as NBC could be used to achieve n-doping. As illustrated in **Figure 1**A, TPS-Nf generates an acid (proton) upon DUV irradiation due to decomposition of the triphenylsulfonium chromophore.[31] The generated proton is then responsible for p-doping of the graphene layer, lowering the Fermi energy level (i.e. shifting farther from the vacuum level, and thereby increasing the work function) (Figure 1C).[32] In the case of the photobase generator NBC, the *o*-nitrobenzyl chromophore follows a known intramolecular rearrangement resulting in the formation of a photochemically liberated free-amine under DUV irradiation (Figure 1B).[30] This free-amine has a lone pair of electrons which we believe are responsible for n- doping of graphene as previously demonstrated in our earlier 3-aminopropyltriethoxysilane (APTES) self-assembled monolayers (SAMs) studies.[24,25] Density functional theory (DFT) calculations have shown that for NH_3 molecules, there is a small charge transfer to the graphene.[33] This would explain the increase of the Fermi level from the Dirac point (i.e. n-doping).[25,34]

Figure 1C shows a simple scheme of a FET device with graphene coated with TPS-Nf or NBC as well as the photochemical induced Fermi energy changes upon exposure of the device. To determine the applicability of our proposed approach, graphene/TPS-Nf and graphene/NBC samples were fabricated using chemical vapor deposition (CVD) grown monolayer graphene transferred onto a 300 nm SiO_2/Si wafer using a common method described elsewhere[24,35] and annealed under an inert atmosphere to remove ambient and transfer process residues[36,37] (i.e. graphene layers that are here after referred as "as-transferred"). For the TPS-Nf treated sample, a 2% solution of TPS-Nf (Sigma Aldrich) dissolved in anhydrous ethanol was spin cast under inert atmosphere onto the as-transferred graphene. For the NBC treated sample, a 2% solution of NBC (Midori Kagaku Co.) dissolved in anhydrous toluene was spin cast in a similar fashion onto as-transferred graphene samples.

Raman spectroscopy was utilized to investigate the quality of the graphene and its doping state by examining the D, G, and 2D bands and their respective peak positions. The "as-transferred" graphene films utilized in this work showed prominent graphitic (G and 2D) (see **Figure 2**a, full spectra) bands with a minimal defect peak (D) (see S.I. Figure S1). The high 2D over G band intensity ratio (I_{2D}/I_G) and low full width at half maximum (FWHM) of the 2D band are indicative of monolayer graphene films.[35]

Figure 2b-d shows the G band position, the G band full width at half maximum (FWHM), the 2D band position and the 2D to G band intensity ratio (I_{2D}/I_G) for as-transferred graphene, the transferred graphene after spin coating with the TPS-Nf or NBC dopants without any further DUV light exposure (hereafter referred as "unexposed"), and finally the transferred graphene after coating with the TPS-Nf or NBC dopants after DUV exposure (5 min exposure for TPS-Nf and 10 min exposure for NBC). For the graphene/TPS-Nf treated sample, the as-transferred and unexposed peak positions remain mostly constant : G peak position of ~1585 cm^{-1}, full width half maximum of the G peak (FWHM) ~20 cm^{-1}, 2D peak position of ~2677 cm^{-1} and I_{2D}/I_G ratio of ~3.2, which indicates that prior to exposure,

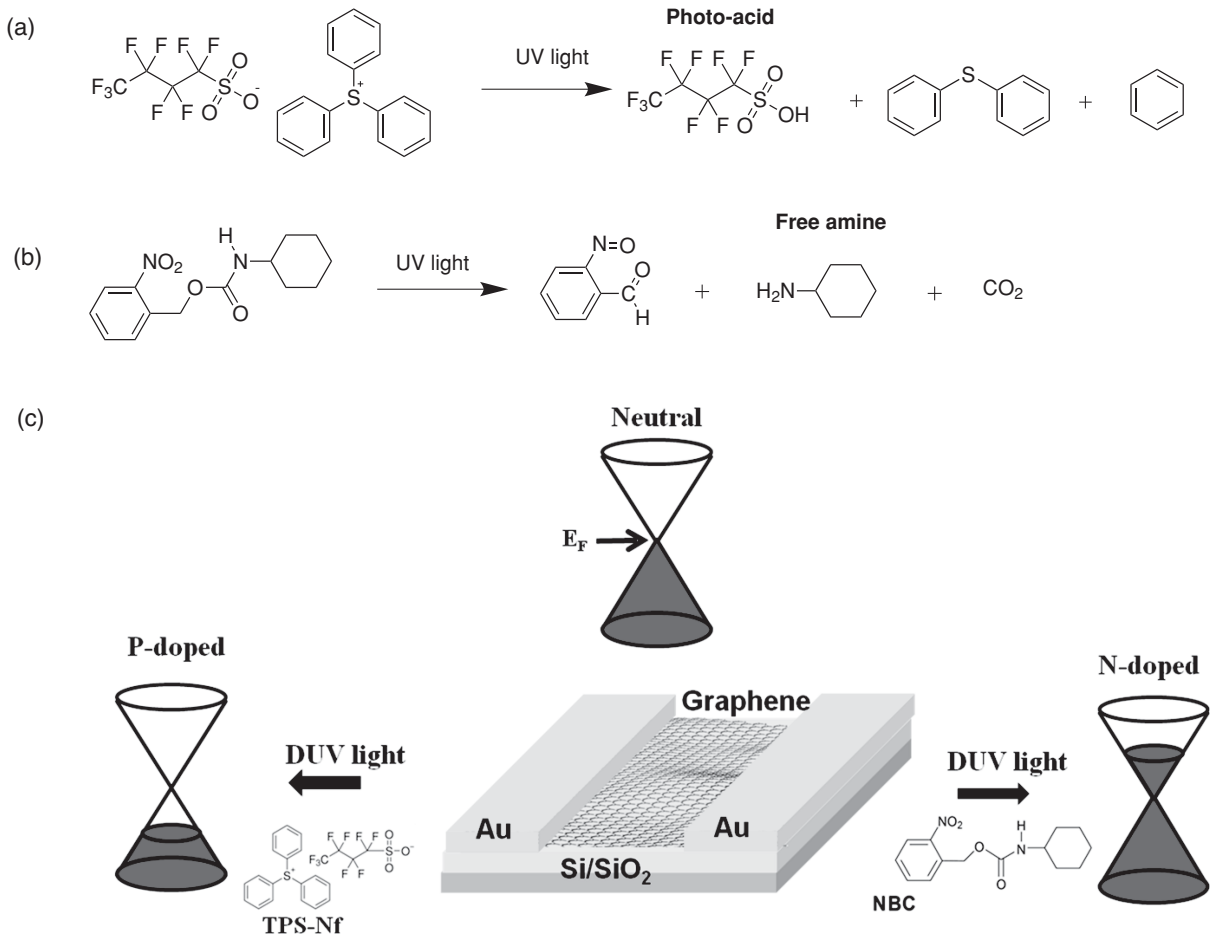

Figure 1. Schematic of reaction pathways for a) TPS-Nf and b) NBC. c) Schematic representation of p- and n-doping of graphene field effect transistor (FET) by TPS-Nf and NBC respectively, with associated changes to the graphene Fermi Energy level.

no significant doping is induced into the graphene by coating of the TPS-Nf onium salt photoacid generator. After exposure however, a clear change in the Raman peak positions and their relative intensities for the sample coated with TPS-Nf PAG is observed: an upshift in the G peak position to ~1608.6 cm^{-1}, a decrease on the FWHM of G peak to ~11.3 cm^{-1}, an upshift in the 2D peak position of ~2690 cm^{-1}, and a decrease in the I_{2D}/I_G ratio to ~0.76, which all are consistent with p-doping of the graphene by the photochemical decomposition of the TPS-Nf to produce photoacid.[20,38] Similarly, for the NBC treated sample, the same behavior is observed where prior to exposure the peak positions remain constant when comparing the as-transferred graphene both coated and not coated with NBC: G peak position of ~1585 cm^{-1}, FWHM of the G peak ~20 cm^{-1}, 2D peak position of ~2675 cm^{-1} and I_{2D}/I_G ratio ~3.2. After exposure, again the graphene sample coated with the NBC exhibits clear changes in the peak positions and their intensity ratios: an upshift in the G peak position to~1596 cm^{-1}, a decrease in the G peak FWHM to~16 cm^{-1}, an upshift in the 2D peak position to ~2678 cm^{-1}, and a decrease in the I_{2D}/I_G ratio to ~2, which are all consistent with n-doping of the graphene.[39] Both of these results obtained by Raman spectroscopy are in clear agreement with the observations by Ferrari and coworkers on n and p-doping of electrochemically top-gated graphene transistor[39] and is further supported by the UPS/XPS and electrical data discussed below.

The p- and n-doping effect of TPS-Nf and NBC respectively, were also evaluated by UV photoelectron spectroscopy (UPS). **Figure 3**A shows the UPS spectra for (1) TPS-Nf and (2) NBC: as-transferred, unexposed and finally after exposure (5 and 10 min for TPS-Nf and NBC respectively). The work function Φ (energy difference between the Fermi and vacuum level) can be calculated from Equation (1),[40] since the secondary electron edge occurs at the binding energy corresponding to the deepest of the energy levels that can be excited with the radiation employed.

$$\Phi = 21.22 - BE_{SEE} \quad (1)$$

where BE_{SEE} is the binding energy at the secondary electron cutoff. The work function of the as-transferred graphene, unexposed graphene/TPS-Nf and graphene/TPS-Nf after exposure were determined to be 3.82 ± 0.1 eV, 3.97 ± 0.1 eV and 5.29 ± 0.09 eV, respectively (Figure 3B). These values are in good agreement with the results obtained from the Raman spectrum where no significant changes were observed in the unexposed graphene/TPS-Nf film as compared to the as-transferred graphene, while after DUV light exposure the graphene

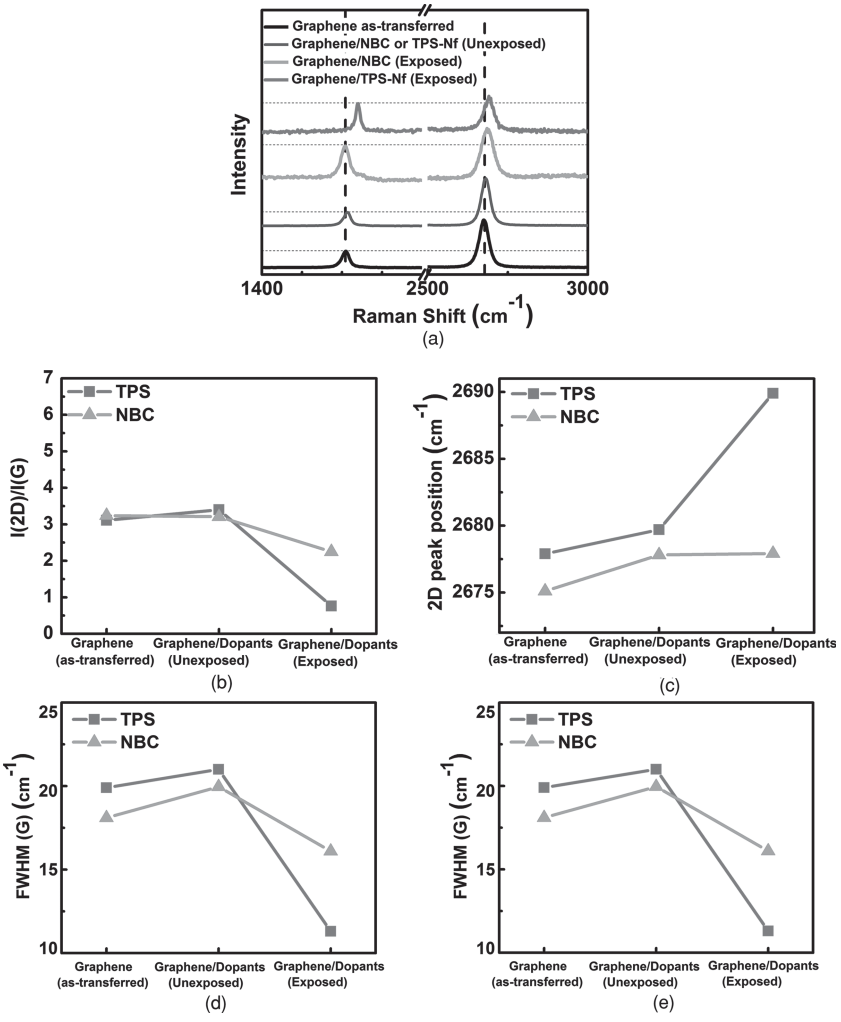

Figure 2. (a) Full Raman spectra for four samples on SiO_2: graphene as-transferred (black line), Graphene/NBC or Graphene/TPS-Nf unexposed (since both yielded the same spectra with no significant changes as compared to the initial graphene spectra) (blue line), Graphene/NBC after exposure (green line) and Graphene/TPS-Nf after exposure (red line). (b) G band peak position, (c) 2D band peak position, (d) FWHM of the G band and (E) ratio of the 2D band peak intensity over G band peak intensities for the samples initially (as-transferred), unexposed and finally after exposure.

exhibits significant p-doping. Using Equation (2), the electron concentration (n) was calculated since it is related to the energy position of the Dirac point by the equation,[41]

$$E_D = h v_F (\pi n)^{-1/2} \quad (2)$$

where v_F is the Fermi velocity of graphene (1.1×10^{-6} ms^{-1}).[42] The calculated doping concentration was approximately 1.2×10^{14} cm^{-2}, which is the highest doping level reported to date for photochemically p-doped graphene and is comparable to the results obtained from other doping techniques.[26,43,44]

Similarly, for NBC, the work function for as-transferred graphene, unexposed graphene/NBC and exposed graphene/NBC were determined to be 3.80 ± 0.07 eV, 3.77 ± 0.11 and 3.38 ± 0.18 eV, respectively, using Equation (1) (Figure 3B). Once again, no significant change was observed in the graphene samples prior to the DUV exposure. Similarly, using Equation (2), the electron concentration (n) was found to be 1.1×10^{13} cm^{-2} after exposure.

Doping of graphene induced by surface electron transfer can further be examined and confirmed by X-ray photoelectron spectroscopy (XPS) measurements. Figure 3C shows the chemical shifts in the high resolution C1s spectra for: (1) as-transferred graphene (black), (2) exposed graphene/TPS-Nf (red) and (3) exposed graphene/NBC (green). It is observed that for the bare graphene sample, the C1s peak maximum occurs with a binding energy (BE) of 284.9 eV as expected.[37,45] For the graphene/TPS-Nf sample, upon on DUV exposure, the C1s peak of graphene shifts to lower binding energy from 284.9 eV to 284.2 eV which is expected for a p-doped sample.[20] For the graphene/NBC sample, the C1s peak has contributions from graphene and the dopant, with an overall maximum shift to higher binding energy from 284.9 eV to 285.9 eV.[23] This is presumably the result of both the BE of the dopant C 1s and the n-doping of graphene by the free-amine present in the NBC layer,[23,46] in accord with previously reported data.[47] It is important to notice that, for the unexposed samples, no shift on the binding energy of the C1s peak was observed (Figure S2 D), in agreement with the UPS and Raman results. N1s and S2s high-resolution spectra for each sample were also collected and the results are presented in the S.I. (S2 A and B). These clearly show that after exposure both molecules undergo the expected photo-reaction: (1) the NBC case shows the emergence of the free amine peak at ~401 eV in the N1s spectra[48] and (2) the TPS-Nf case shows the appearance of the peak at ~227.5 eV in the S2s spectra that is attributed to the rearrangement of the sulfur center in the TPS salt after the photoacid generation.[49] These results further support our statement concerning p–type and n-type doping observed for TPS-Nf and NBC coated graphene films.

Once evidence of doping using photochemically activated PAG and PBG compounds was obtained, the next step was to quantify the effect of such doping strategies on the electrical properties of graphene. In order to test the electrical transport properties of graphene that has been modified using such photochemically activated dopants, back-gated graphene field effect transistors (GFET) were fabricated using standard lithography and metallization techniques reported previously.[24,25]

Figure 4 shows the resulting drain current (I_d) versus the gate voltage (V_g) for TPS-Nf and NBC coated graphene films. For the bare, as-transferred graphene, all devices demonstrated a charge neutrality point (V_{NP}) of approximately zero volts as a

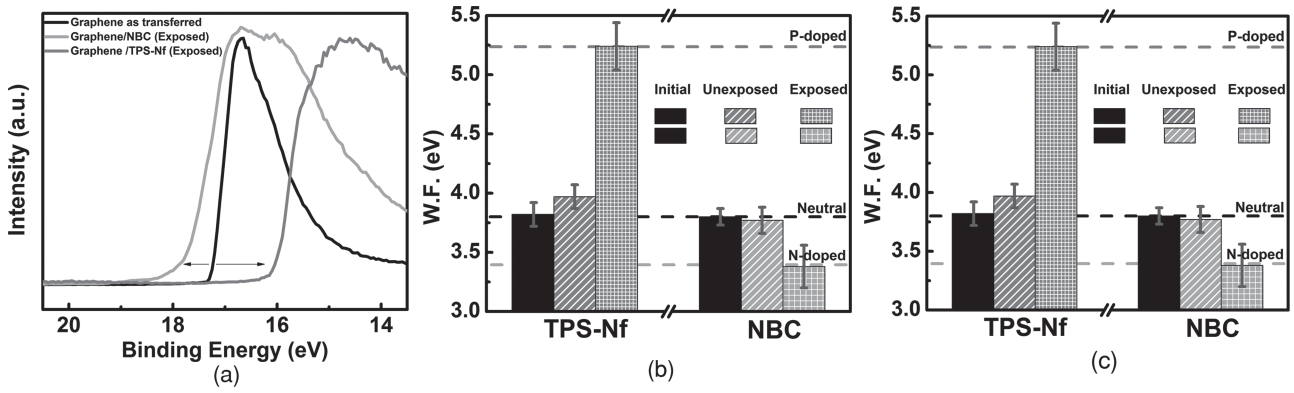

Figure 3. (a) UPS spectra for Graphene as-transferred (black), Graphene/TPS-Nf exposed (red) and Graphene/NBC exposed (green), (b) UPS-determined work functions. XPS spectra representing the (c) C1s binding energy region for three types of samples: graphene as-transferred (black line), graphene/TPS-Nf (red line) and graphene/NBC (green line) exposed on SiO_2. All data were normalized to the largest intensity within each spectrum.

result of the careful washing in multiple acetone baths followed by a 30 min anneal at 200 °C under a nitrogen environment to remove any adsorbed p-dopants from the transfer process of the CVD graphene.[37] The annealing time and temperature were controlled carefully in order to avoid n-doping as previously reported.[50] For the GFET devices made using TPS-Nf (Figure 4A), a shift in the neutrality point of ~−15 V was observed in unexposed films, which is attributed to ethanol[51] exposure during the TPS-NF coating process as shown in our control experiment. Figure S3 in the S.I. shows that a drop of ~−15 V in the neutrality point was observed for a graphene sample dipped in ethanol and immediately dried with nitrogen, which clearly demonstrates solvent induced n-doping similar to that observed in the TPS-Nf coating case.

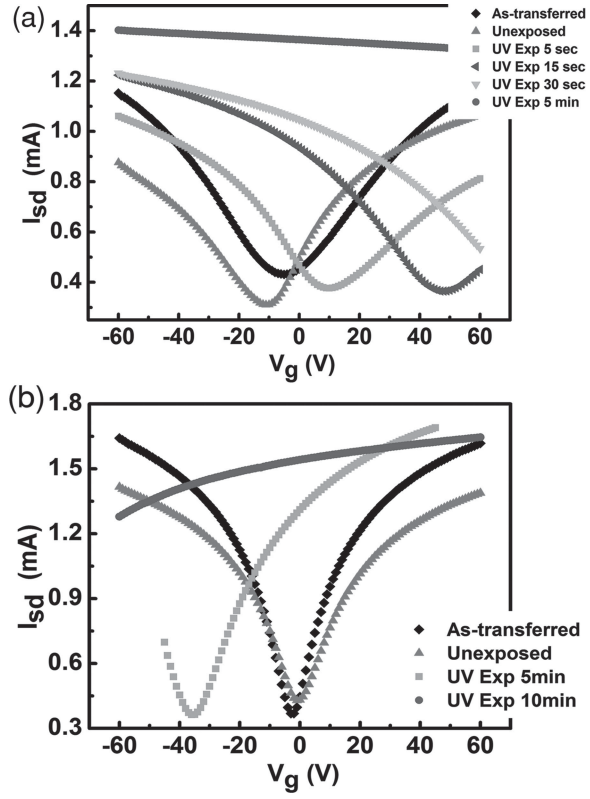

Figure 4. Source-drain current versus gate voltage for a simple graphene FET device for (a) graphene/TPS-Nf and (b) graphene/NBC. (Vsd = .1V).

Upon exposure of the TPS-Nf coated graphene film devices, the charge neutrality point is observed to gradually shift to higher voltages as would be expected for increasing levels of p-doping with increasing exposure time and generation of additional photoacid. At 5 s exposure, the neutrality point shifts to ~10 V; at 15 s, the neutrality point stabilized at ~48 V; for 30 s it is above 60 V and after 5 min, the charge neutrality point is so far beyond 100 V that it is difficult to resolve with the available measurement techniques. The hole concentration (n) of the TPS-Nf treated graphene after annealing was calculated from the V_{NP} using Equation (3),[52]

$$n = C_G V_{NP} / e \tag{3}$$

where C_G = 115 aF/μm^2,[52] e is the charge of the electron, and V_{NP} is the voltage at the charge neutrality point. Hole concentrations were calculated to be approximately 7.19×10^{11} cm^{-2} and 3.45×10^{12} cm^{-2} for the 5 s and 15 s exposure respectively (i.e. these were the only cases where the neutrality point could be precisely measured because of the voltage limitations of the probe measurement system used). The electron concentration (n) is related to the energy position of the Dirac point by Equation (2), hence the calculated energy position of the Dirac point, were approximately 0.11 eV and 0.24 eV after 5 and 15 s exposure respectively.

Figure 4b shows the electrical response for the GFET devices made using NBC. In the unexposed state, little shift in the neutrality point is observed. This lack of a shift in the neutrality point is indicative of a lack of chemical doping of the graphene by NBC or the toluene solvent used to coat it onto the GFET device (Figure S4). This is consistent with earlier observations made in the Raman spectroscopy and UPS data. Upon exposure of the NBC-coated GFET, the charge neutrality point is observed to gradually shift to lower voltages with increasing exposure time and generation of larger amounts of photobase. At 5 min, the neutrality point stabilizes at ~−36 V and after 10 min, the charge neutrality point is far above 60 V which

is the maximum amount of voltage that can be applied to the device using the tool configuration. The electron concentration (n) of the NBC-treated graphene after annealing is approximately 2.58×10^{12} cm^{-2} for the 5 min exposure as calculated using Equation (2) and the energy position of the Dirac point is approximately 0.20 eV as calculated from Equation (3). One of the reasons NBC requires a higher exposure time than TPS-Nf (10 s versus 5 min) in order to observe a change in the doping concentration, rises from the fact that the quantum yield (Q) (the ratio of product molecules, photoacid for TPS-Nf or photobase for NBC, to absorbed photons), for TPS-Nf is approximately five times higher than NBC (0.52 versus 0.1).[30,31] Nevertheless the electrical measurements are in agreement with the Raman, UPS and XPS results which clearly indicate that prior to exposure, there is little effect on the V_{NP} for graphene and that after exposure both TPS-Nf and NBC p- and n-dope respectively. The field-effect mobility for both holes (h) and electrons (e) of the devices was extracted using Equation (4),[9]

$$\mu = L_{ch} g_m / W_{ch} V_{ds} C_{ox} \quad (4)$$

where μ = mobility, L_{ch} = 2000 μm, $g_m = dI_D/dV_{GS}$, W_{ch} = 50 μm, V_{DS} = 0.1 V and Cg = 115 aF/μm^2. For an untreated GFET made using the graphene films used to later manufacture the TPS-Nf doped GFETs (i.e. simply measured before treatment with TPS-Nf PAG), the extracted mobilities were in the range of ~400 cm^2/Vs (h) and ~350 cm^2/Vs (e). For the unexposed TPS-Nf treated GFET, the extracted mobilities were ~350 cm^2/Vs (h) and ~500 cm^2/Vs (e). After exposure of the TPS-Nf PAG coated device to 5 sec of DUV light, the mobilities of the GFET were measured to be ~390 cm^2/Vs (h) and 300 cm^2/Vs (also we are unable to observe the neutrality point clearly after 5 s exposure).

For an untreated GFET made using the graphene films used to later manufacture the NBC doped GFETs (i.e. simply measured before treatment with NBC), the extracted mobilities were in the range of ~1200 cm^2/Vs (h) and ~1200 cm^2/Vs (e). For the unexposed NBC treated GFET, the extracted mobilities were ~900 cm^2/Vs (h) and 850 cm^2/Vs (e). After exposure of the NBC coated device to 5 s of DUV light, the mobilities of the GFET were measured to be ~900 cm^2/Vs (h) and 950 cm^2/Vs. As expected for the type of dopants used in this work where we have a high carrier density in graphene after charge transfer, there is in general a decrease in the mobility of the graphene vis-à-vis pristine graphene which is due to enhanced short-range scattering.[21,44,53] It is important to mention that the variation in the mobilities between the untreated graphene films used to fabricate the PAG and PBG treated GFETs were due to variation from normal graphene to graphene film variations observed in different batches of as-transferred graphene after synthesis, transfer, and processing onto device wafers. Nevertheless, the Raman for both samples showed no defect bands and these mobility differences in the starting graphene films are not expected to affect the doping mechanisms of both the PAG and PBG.

Using Equation (3), the expected V_{NP} was calculated for both TPS-Nf and NBC photoinduced doping from the work function values determined via UPS on exposed graphene/TPS-Nf and graphene/NBC samples. The estimated neutrality point positions were 148 V for NBC (10 min exposure) and 1700 V for TPS-Nf. These estimates were in general agreement with the GFET electrical measurements since the neutrality point for both exposure times was far above 100 V (Figure 4). An increase in device current magnitude (at Vg = 0) of 3 to 5 times was also observed, which also indicated that the conductivity of the device was being improved in a similar manner (Figure 4). In this case, such changes were achieved while maintaining film transmittance above ~70% for both dopants (Figure S5). Experiments are underway that focus on improving and optimizing such parameters which are sought in a variety of applications.[5] Air stability for the samples prior to exposure was also tested (Figure S6 and S7 S.I.) and showed slight to no decrease in the neutrality point of the graphene-coated samples, in contrast to the bare graphene exposed to air (S.I. Figure S8). This shows that the PAG and PBG dopant precursor layers can protect the graphene quality at least to some degree, presumably by acting as a water and oxygen barrier, until the films are exposed to generate the desired doping. This is in contrast to other doping techniques that require further annealing in order to remove such atmospheric dopants.[13,23,24] It is important to mention that after DUV light exposure, subsequent air exposure of the doped graphene films did not maintain the desired doping, presumably due to neutralization of the photogenerated acid or base species, and thus a protective layer or packaging should be used in such cases or they should be handled under an inert atmosphere.

In order to demonstrate the ability to develop an area-selected pattern-wise doping, back-gated graphene-based p-n junction with patterned p-n regions in the FET channel were fabricated using TPS-Nf as dopant and were measured following the same basic process described above. First, 50 nm thick gold electrodes were evaporated through a shadow mask onto a clean, graphene transferred, 300 nm thick SiO_2 gate dielectric films on highly p-doped silicon wafers. Next, half of each of the channels in the FET devices were covered with a shadow mask and exposed to DUV light (**Figure 5**a).

The area selectivity of the chemical conversion of the PAG dopant precursor in the patterned FET device was confirmed by XPS mapping of the FET as illustrated in Figure 5b and c. The signal at a binding energy of 163 eV was used for mapping the S2p spectra, which is associated with the exposed TPS-Nf as discussed earlier (Figure S2). The Figure 5b shows a well defined boundary in the S2p spectral map of the FET, as quantified by the signal intensity at 163 eV over the area of the device, between areas of the substrate that were exposed to DUV light and those left unexposed. C1s mapping of the photopatterned FET devices was also accomplished (Figure 5c) as quantified by the signal intensity at a binding energy of 284 eV, which corresponds to p-doped graphene (Figure 3). Again, a well-defined boundary in the doping of the FET channel was observed, with the exposed regions of the FET channel showing clear signs of p-doping. Furthermore, the areas of the FET device exhibiting the most intense C1s signal at 284 eV which is indicative of p-doping, were perfectly correlated with the areas of the device exhibiting the strongest S2p signal that is indicative of the production of the photoacid as well. All of these results are consistent with the formation of a well defined photopatterned p-doped region that is the result of exposure induced production of photoacid dopant in selected portions of the FET channel.

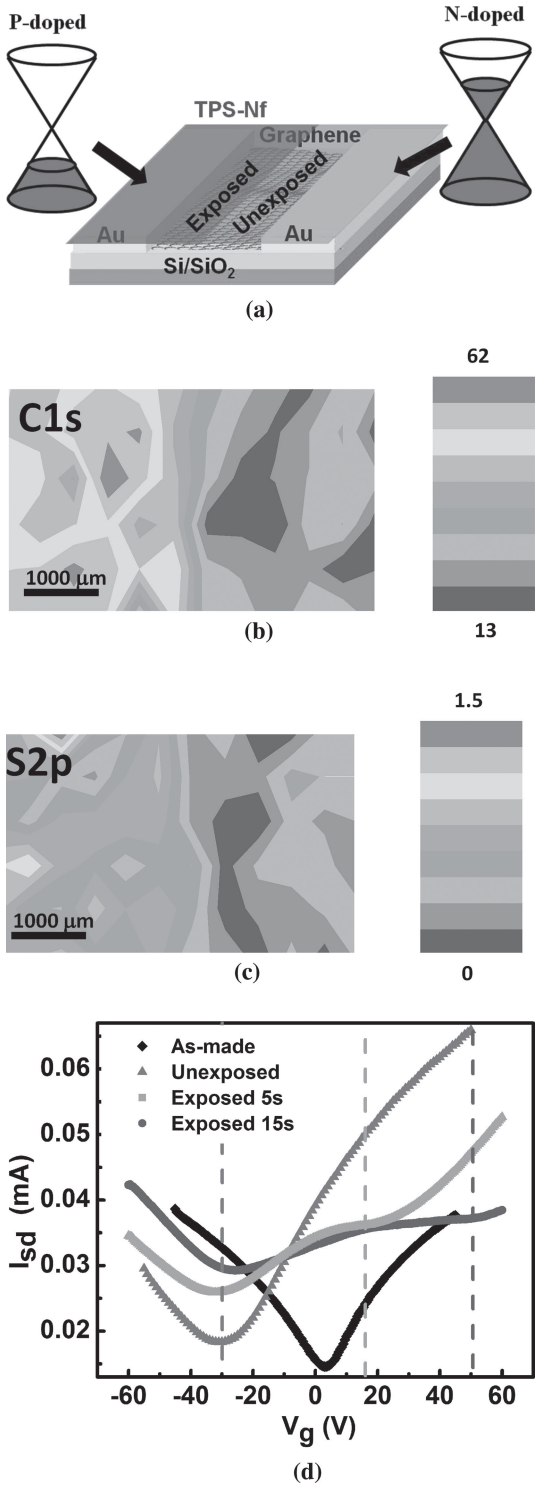

Figure 5. (a) Schematic showing the fabricate graphene/TPS-Nf p-n junction. XPS mapping of the graphene p-n junction for the (b) C1s intensity at a binding energy of ~ 284 eV (c) S2p intensity at a binding energy of ~163 eV. (d) Source-drain current versus gate voltage as a function of exposure time for a graphene p-n junction (Vsd = 5 V).

Electrical measurements were performed on the fabricated CVD graphene devices containing the photopatterned TPS-Nf dopant precursor coatings. The devices were probed under inert atmosphere using a method similar to that described earlier. As expected, the unexposed sample exhibited a slight n-type characteristic due to the solvent (Figure 5c and S3) processing with only a single obvious neutrality point. For devices with a 5 s ultraviolet exposure through the shadow mask on the device channel, two minima in the Isd-Vg data were clearly observed, corresponding to two neutrality points as would be expected from a p-n junction,[12,25,28] which in this case is formed by the photochemically created p-type doped region in the slightly n-type device layer. For devices with a 15 s masked ultraviolet exposure of the channel, again two minima are clearly observed in the Isd-Vg data and additionally the positive Vg neutrality point shifts to more positive values as would be consistent with higher doping levels that result from further photoacid generation during the longer exposure. It is important to notice that the position of the neutrality points in the p-n junction are in agreement with the expected position obtained and discussed earlier from the blanket film exposure experiments (~12 V and 50 V for 5 s and 15 s exposure respectively of TPS-Nf coated graphene samples) and that little change is observed in the position of the Dirac point corresponding to the unexposed slightly n-type region. It was also possible during these measurements to demonstrate the unique ambipolar character of the devices. Switching of the source-drain bias voltage from positive to negative values showed no rectifying behavior as would be characteristic of an ambipolar device.[12,54] This unique p-n junction behavior of graphene, in contrast with the traditional rectifying behavior of conventional semiconductors, allows the development of graphene-based bipolar devices which have been demonstrated to display new and exciting phenomena such as Klein tunneling,[55,56] and produce lensing effects for coherent electrons, i.e. so called Veselago lensing.[57] Our simple method for producing patterned doping profiles in graphene films and devices facilitates the study of such phenomena and possibly enables the use of graphene for a variety of applications such as circuits and sensors, since it allows precise, simple and independent control over the work function and doping properties of graphene, as compared to the more limited and difficult control possible with electrostatic substrate engineering,[12] and other fabrication techniques.[55,58]

3. Conclusion

In the work reported here, we have developed an on-demand photochemical method for doping of graphene using triphenylsulfonium perfluoro-1-butanesufonate (TPS-Nf) and 2-nitrobenzyl *N*-cyclohexylcarbamate (NBC) photoacid and photobase generators. Both compounds can be used to easily dope graphene and such doping can be controlled in an area-selective manner using traditional lithographic exposure techniques and tools. Electrical measurements and XPS confirm that before exposure, graphene coated with either TPS-Nf or NBC maintains its pristine electrical properties, and that by modulating the deep ultraviolet (DUV) light exposure dose delivered to the films, the doping concentration for both p and n-type doping can be easily modulated and controlled. This doping technique yields a possible work function modulation from 3.4 eV to 5.3 eV in single layer graphene. Area-selective

doping and modification of an existing graphene FET device are demonstrated through photochemical formation of a p-n junction in a pre-fabricated graphene FET device coated with TPS-Nf and exposed in a pattern-wise manner. The exposure is masked in such a way that the p-n junction is formed in the middle of the graphene FET device channel. Measurements of the I-V characteristics of the photochemically doped FET device show the expected two current minima (i.e. two Dirac or neutrality points) for an ambipolar p-n junction in graphene. Our simple method for producing patterned doping profiles in graphene films and devices opens up a variety of new possibilities for forming complex doping profiles in a simple manner in graphene, and can enable rapid testing of concepts for graphene devices involving controlled work function tuning, complex doping profiles and simple post-fabrication tuning of devices.

4. Experimental Section

Graphene Growth: CVD graphene was obtained following standard literature procedures.[35] Graphene was synthesized on 25 μm thick Cu foil (Alfa Aesar, item No. 14482, cut into 1 × 1 in squares) in a low pressure $Ar/H_2/CH_4$ environment at 1000 °C.[35] PMMA (MicroChem 950 PMMA Series) was spun cast from an organic solution (9% solution by weight in anisole, spin coated at 1500 rpm for 1 min) onto the as-grown graphene coated Cu samples and baked (180 °C for 10 min) to form an approximately 500 nm thick film that served as an auxiliary support material for handling and transferring the graphene films. The sample was treated overnight with a 30 wt% $FeCl_3$ aqueous solution to remove the copper foil. The resulting bi-layer PMMA-graphene samples were treated with 10 wt% HCl solution for 10 min, followed by deionized (DI) water several times to remove bound contaminants. The PMMA-graphene bilayers were then placed onto SiO_2 coated Si substrate with the graphene face in contact with the SiO_2 surface. The PMMA carrier film was then removed by immersing the substrate film stack in fresh acetone up to 5 times for 30 min each time. Finally the graphene/SiO_2/Si stacks were annealed at 200 °C under an inert nitrogen or argon atmosphere for 10 min. The samples were then analyzed by Raman and XPS to ensure the successful removal of the copper and PMMA films and the presence of clean mono-layer graphene films.

Device Fabrication, Doping Procedure, and Electrical Measurements: A highly p-doped Si wafer was as the substrate for field effect device fabrication since it could be easily used as a common gate for all devices. A 300 nm thick thermal silicon dioxide layer grown on the p-doped Si wafers was used as the gate dielectric. The Si/SiO_2 substrate was cleaned by piranha solution and pre-treated by UV ozone for 15 min. Next, lithography and deposition processes (i.e. typical lift-off procedures) were used to form the gold electrodes (3 nm thick chromium adhesion layer first deposited onto the SiO_2 followed by a 50 nm thick gold layer for electrode fabrication, where width = 50 μm and length = 2000 μm) on the 300 nm thick SiO_2 gate dielectric. Monolayer graphene was transferred to these pre-fabricated electrode devices using the procedure described earlier. For n-doping, samples were coated with NBC via spin casting (1000 rpm for 1 min) using a 2% v/v solution of NBC in anhydrous toluene. For p-doping the samples were coated with TPS-Tf via spin casting (1000 rpm for 1 min) using a 2% v/v solution of TPS-Nf in anhydrous ethanol. The samples were exposed using a handheld DUV light (Model UVGL-25: 4 watt UV lamp, wavelength 254 nm) for a time period varying from (10 s to 10 min). Once the electrode devices were fabricated, all the sample preparations beginning with the graphene transfer were performed inside of a glovebox in a controlled environment. Electrical measurements, including I-V curves, were made using a probe station configured with a HP 4156 semiconductor parameter analyzer maintained under an inert atmosphere in the glovebox as well. A control sample containing only graphene that was exposed to DUV was also analyzed to confirm that any changes in the neutrality point are in fact a result of the dopants (Figure S9).

For p-n junction fabrication, 50 nm thick gold electrodes (3 nm thick chromium was used for adhesion, width = 5000 μm, length = 10 000 μm) were evaporated through a shadow mask onto a clean, graphene transferred, 300 nm thick SiO_2 gate dielectric films on highly p-doped silicon wafers. TPS-Nf was spin-coated following the same conditions mentioned above; half of each of the channels in the FET devices were covered with a shadow mask, exposed to DUV light and measured following the same basic process described above.

Surface Characterization and UV/Visible Spectroscopy: Transfers from the glovebox into the photoelectron spectrometer were done under N_2 atmosphere using a Kratos air-sensitive transporter 39–322 that couples into the transfer chamber of a Kratos Axis Ultra^{DLD} XPS/UPS system under positive N_2 pressure. All samples were in electronic equilibrium with the spectrometer via a metallic clip on the graphene and characterizations were performed at normal take-off angle. XPS using monochromatic Al Kα line was performed at a base pressure of 10^{-9} Torr with the Fermi level calibrated using atomically clean silver. Spot size was ca. 700 μm. Survey XPS scans were run at 160 eV pass energy and high resolution scans typically at 20 eV pass energy and 100 meV steps, while UPS spectra were acquired at 5 eV pass energy and 0.05 eV step size with the aperture and iris set to 55 μm . Calibration of spectra was done with the Si 2p peak set to BE = 104.9 eV, same as that of the treated graphene (10 min) on SiO_2. XPS mapping was acquired using a Thermo K-Alpha XPS (Thermoscientific) operating under ultra-high vacuum conditions with an Al Kα micro-focused monochromator and a 30 μm spot size. Raman spectroscopy and microscopy measurements were performed using a Horiba HR800 μRaman system without exposure to air.[37] All spectra were excited with visible (532 nm) laser light and collected in a backscattering configuration with a laser power below 0.5 mW to reduce laser-induced heating and were acquired at multiple locations to verify reproducibility. All the peaks were fitted with Gauss-Lorentzian curve fits to determine their peak position, line width, and intensity.

UV/Visible spectroscopy was acquired in an Agilent Cary 5000 UV/Vis spectrometer for 0.5 cm radius spots (under air). Glass was used as the sample and reference to calibrate the 100%T, and 0%T was calibrated by blocking the sample light path. CVD graphene was transferred to the same type of glass slides and annealed in the glovebox at 200 °C before treatment.

Supporting Information

Supporting Information is available from the Wiley Online Library or from the author.

Acknowledgements

The authors would like to gratefully acknowledge the National Science Foundation for support of this work through grants CHE-0822697, CHE-0848833 and the Georgia Tech MRSEC program, DMR-0820382 and CMMI-0927736 for generous support of this work.

Received: November 8, 2013
Revised: December 20, 2013
Published online: June 4, 2014

[1] A. K. Geim, *Science* **2009**, *324*, 1530.
[2] a) K. S. Novoselov, A. K. Geim, S. V. Morozov, D. Jiang, Y. Zhang, S. V. Dubonos, I. V. Grigorieva, A. A. Firsov, *Science* **2004**, *306*, 666; b) S. K. Pati, T. Enoki, C. N. R. Rao, *Graphene and its Fascinating Attributes* World Scientific, Singapore, Hackensack, N.J. **2011**; c) A. H. Castro Neto, F. Guinea, N. M. R. Peres, K. S. Novoselov, A. K. Geim, *Rev. Mod. Phys.* **2009**, *81*, 109.

[3] A. K. Geim, K. S. Novoselov, *Nat. Mater.* **2007**, *6*, 183.
[4] G. Jo, M. Choe, S. Lee, W. Park, Y. H. Kahng, T. Lee, *Nanotechnology* **2012**, 23.
[5] K. S. Novoselov, V. I. Fal'ko, L. Colombo, P. R. Gellert, M. G. Schwab, K. Kim, *Nature* **2012**, *490*, 192.
[6] J. K. Wassei, R. B. Kaner, *Accounts Chem. Res.* **2013**, *46*, 2244.
[7] a) A. Kasry, M. A. Kuroda, G. J. Martyna, G. S. Tulevski, A. A. Bol, *ACS Nano* **2010**, *4*, 3839; b) K. S. Kim, Y. Zhao, H. Jang, S. Y. Lee, J. M. Kim, J. H. Ahn, P. Kim, J. Y. Choi, B. H. Hong, *Nature* **2009**, *457*, 706; c) Z. K. Liu, J. H. Li, Z. H. Sun, G. A. Tai, S. P. Lau, F. Yan, *ACS Nano* **2012**, *6*, 810.
[8] Y. Shi, K. K. Kim, A. Reina, M. Hofmann, L. J. Li, J. Kong, *ACS Nano* **2010**, *4*, 2689.
[9] F. Schwierz, *Nat. Nano* **2010**, *5*, 487.
[10] a) Y. M. Lin, C. Dimitrakopoulos, K. A. Jenkins, D. B. Farmer, H. Y. Chiu, A. Grill, P. Avouris, *Science* **2010**, *327*, 662; b) T. H. Han, Y. Lee, M. R. Choi, S. H. Woo, S. H. Bae, B. H. Hong, J. H. Ahn, T. W. Lee, *Nat. Photonics* **2012**, *6*, 105.
[11] V. Georgakilas, M. Otyepka, A. B. Bourlinos, V. Chandra, N. Kim, K. C. Kemp, P. Hobza, R. Zboril, K. S. Kim, *Chem. Rev.* **2012**, *112*, 6156.
[12] H. Y. Chiu, V. Perebeinos, Y. M. Lin, P. Avouris, *Nano Lett.* **2010**, *10*, 4634.
[13] H. Liu, Y. Liu, D. Zhu, *J. Mater. Chem.* **2011**, *21*, 3335.
[14] D. Usachov, O. Vilkov, A. Gruneis, D. Haberer, A. Fedorov, V. K. Adamchuk, A. B. Preobrajenski, P. Dudin, A. Barinov, M. Oehzelt, C. Laubschat, D. V. Vyalikh, *Nano Lett.* **2011**, *11*, 5401.
[15] S. A. Paniagua, J. Baltazar, H. Sojoudi, S. K. Mohapatra, S. Zhang, C. L. Henderson, S. Graham, S. Barlow, S. R. Marder, *Mater. Horizons* **2014**, *1*, 111.
[16] R. A. Nistor, D. M. Newns, G. J. Martyna, *ACS Nano* **2011**, *5*, 3096.
[17] W. Chen, D. C. Qi, X. Y. Gao, A. T. S. Wee, *Prog. Surf. Sci.* **2009**, *84*, 279.
[18] Y. C. Lin, C. Y. Lin, P. W. Chiu, *Appl. Phys. Lett.* **2010**, 96.
[19] S. Huh, J. Park, K. S. Kim, B. H. Hong, S. Bin Kim, *ACS Nano* **2011**, *5*, 3639.
[20] W. H. Lee, J. W. Suk, J. Lee, Y. F. Hao, J. Park, J. W. Yang, H. W. Ha, S. Murali, H. Chou, D. Akinwande, K. S. Kim, R. S. Ruoff, *ACS Nano* **2012**, *6*, 1284.
[21] D. B. Farmer, R. Golizadeh-Mojarad, V. Perebeinos, Y. M. Lin, G. S. Tulevski, J. C. Tsang, P. Avouris, *Nano Lett.* **2009**, *9*, 388.
[22] a) S. A. Paniagua, J. Baltazar, H. Sojoudi, S. K. Mohapatra, S. Zhang, C. L. Henderson, S. Graham, S. Barlow, S. R. Marder, *Mater. Horizonts* **2014**; b) R. Wang, S. Wang, D. Zhang, Z. Li, Y. Fang, X. Qiu, *ACS Nano* **2010**, *5*, 408.
[23] P. Wei, N. Liu, H. R. Lee, E. Adijanto, L. Ci, B. D. Naab, J. Q. Zhong, J. Park, W. Chen, Y. Cui, Z. Bao, *Nano Lett.* **2013**, *13*, 1890.
[24] J. Baltazar, H. Sojoudi, S. A. Paniagua, J. Kowalik, S. R. Marder, L. M. Tolbert, S. Graham, C. L. Henderson, *J. Phys. Chem. C* **2012**, *116*, 19095.
[25] H. Sojoudi, J. Baltazar, L. M. Tolbert, C. L. Henderson, S. Graham, *ACS Appl. Mater. Inter.* **2012**, *4*, 4781.
[26] a) H. B. M. Shashikala, C. I. Nicolas, X. Q. Wang, *J. Phys. Chem. C* **2012**, *116*, 26102; b) A. R. Jang, E. K. Jeon, D. Kang, G. Kim, B. S. Kim, D. J. Kang, H. S. Shin, *ACS Nano* **2012**, *6*, 9207; c) N. Peimyoo, J. W. Li, J. Z. Shang, X. N. Shen, C. Y. Qiu, L. H. Xie, W. Huang, T. Yu, *ACS Nano* **2012**, *6*, 8878; d) Z. T. Luo, N. J. Pinto, Y. Davila, A. T. C. Johnson, *Appl. Phys. Lett.* **2012**, 100; e) M. Kim, N. S. Safron, C. H. Huang, M. S. Arnold, P. Gopalan, *Nano Lett.* **2012**, *12*, 182.
[27] M. Z. Iqbal, S. Siddique, M. W. Iqbal, J. Eom, *J. Mater. Chem. C* **2013**, *1*, 3078.
[28] Y. D. Kim, M. H. Bae, J. T. Seo, Y. S. Kim, H. Kim, J. H. Lee, J. R. Ahn, S. W. Lee, S. H. Chun, Y. D. Park, *ACS Nano* **2013**, *7*, 5850.
[29] a) R. A. Lawson, L. M. Tolbert, C. L. Henderson, *J. Vac. Sci. Technol. B* **2010**, *28*, C6s12; b) R. A. Lawson, D. E. Noga, L. M. Tolbert, C. L. Henderson, *J. Micro-Nanolith. Mem.* **2009**, *8*, 043010; c) R. A. Lawson, C. T. Lee, L. M. Tolbert, C. L. Henderson, *Microelectron. Eng.* **2009**, *86*, 738; d) R. A. Lawson, C. T. Lee, R. Whetsell, W. Yueh, J. Roberts, L. Tolbert, C. L. Henderson, *Adv. Resist Mater. Process. Technol. XXIV* **2007**, *6519*, N5191.
[30] J. V. Crivello, K. Dietliker, *Photoinitiators for Free Radical Cationic and Anionic Photopolymerization*, *vol. 3*, John Wiley and Sons, London **1998**.
[31] S. Tagawa, S. Nagahara, T. Iwamoto, M. Wakita, T. Kozawa, *Adv. Resist Technol. Process. XVII*, Parts 1 and 2 **2000**, *3999*, 204.
[32] A. Kasry, M. A. Kuroda, G. J. Martyna, G. S. Tulevski, A. A. Bol, *ACS Nano* **2010**, *4*, 3839.
[33] O. Leenaerts, B. Partoens, F. M. Peeters, *Microelectron. J.* **2009**, *40*, 860.
[34] a) K. Yokota, K. Takai, T. Enoki, *Nano Lett.* **2011**, *11*, 3669; b) X. M. Wang, J. B. Xu, C. L. Wang, J. Du, W. G. Xie, *Adv. Mater.* **2011**, *23*, 2464; c) S. Kobayashi, T. Nishikawa, T. Takenobu, S. Mori, T. Shimoda, T. Mitani, H. Shimotani, N. Yoshimoto, S. Ogawa, Y. Iwasa, *Nat. Mater.* **2004**, *3*, 317.
[35] X. Li, W. Cai, J. An, S. Kim, J. Nah, D. Yang, R. Piner, A. Velamakanni, I. Jung, E. Tutuc, S. K. Banerjee, L. Colombo, R. S. Ruoff, *Science* **2009**, *324*, 1312.
[36] S. Ryu, L. Liu, S. Berciaud, Y. J. Yu, H. T. Liu, P. Kim, G. W. Flynn, L. E. Brus, *Nano Lett.* **2010**, *10*, 4944.
[37] H. Sojoudi, J. Baltazar, C. Henderson, S. Graham, *J. Vac. Sci. Technol. B* **2012**, 30.
[38] A. Das, S. Pisana, B. Chakraborty, S. Piscanec, S. K. Saha, U. V. Waghmare, K. S. Novoselov, H. R. Krishnamurthy, A. K. Geim, A. C. Ferrari, A. K. Sood, *Nat. Nanotechnol.* **2008**, *3*, 210.
[39] A. Das, S. Pisana, B. Chakraborty, S. Piscanec, S. K. Saha, U. V. Waghmare, K. S. Novoselov, H. R. Krishnamurthy, A. K. Geim, A. C. Ferrari, A. K. Sood, *Nat. Nano* **2008**, *3*, 210.
[40] H. Ishii, K. Sugiyama, E. Ito, K. Seki, *Adv. Mater.* **1999**, *11*, 972.
[41] Y. B. Zhang, V. W. Brar, F. Wang, C. Girit, Y. Yayon, M. Panlasigui, A. Zettl, M. F. Crommie, *Nat. Phys.* **2008**, *4*, 627.
[42] J. Park, W. H. Lee, S. Huh, S. H. Sim, S. B. Kim, K. Cho, B. H. Hong, K. S. Kim, *J. Phys. Chem. Lett.* **2011**, *2*, 841.
[43] a) Z. Y. Chen, I. Santoso, R. Wang, L. F. Xie, H. Y. Mao, H. Huang, Y. Z. Wang, X. Y. Gao, Z. K. Chen, D. G. Ma, A. T. S. Wee, W. Chen, *Appl. Phys. Lett.* **2010**, 96; b) Y. Qi, U. Mazur, K. W. Hipps, *RSC Adv.* **2012**, *2*, 10579.
[44] S. Tongay, K. Berke, M. Lemaitre, Z. Nasrollahi, D. B. Tanner, A. F. Hebard, B. R. Appleton, *Nanotechnology* **2011**, 22.
[45] S. Bae, H. Kim, Y. Lee, X. F. Xu, J. S. Park, Y. Zheng, J. Balakrishnan, T. Lei, H. R. Kim, Y. I. Song, Y. J. Kim, K. S. Kim, B. Ozyilmaz, J. H. Ahn, B. H. Hong, S. Iijima, *Nat. Nanotechnol.* **2010**, *5*, 574.
[46] P. Chirakul, V. H. Perez-Luna, G. P. Lopez, P. D. Hampton, *Abstr. Pap. Am. Chem. S.* **1999**, *217*, U668.
[47] K. Yokota, K. Takai, T. Enoki, *Nano Lett.* **2011**, *11*, 3669–3675.
[48] W.-M. Yeh, R. A. Lawson, L. M. Tolbert, C. L. Henderson, *SPIE Proceedings* **2012**, *8325*, 83251X.
[49] T. Kumada, Y. Tanaka, A. Ueyama, S. Kubota, H. Koezuka, T. Hanawa, H. Morimoto, *Adv. Resist Technol. Process. X* **1993**, *1925*, 31.
[50] K. Brenner, R. Murali, *Appl. Phys. Lett.* **2011**, 98.
[51] a) F. Schedin, A. K. Geim, S. V. Morozov, E. W. Hill, P. Blake, M. I. Katsnelson, K. S. Novoselov, *Nat. Mater.* **2007**, *6*, 652; b) F. B. Rao, H. Almumen, Z. Fan, W. Li, L. X. Dong, *Nanotechnology* **2012**, 23.
[52] a) Z. X. Shen, Z. H. Ni, H. M. Wang, Z. Q. Luo, Y. Y. Wang, T. Yu, Y. H. Wu, *J. Raman Spectroscopy* **2010**, *41*, 479; b) A. Nourbakhsh, M. Cantoro, A. Klekachev, F. Clemente, B. Soree, M. H. van der Veen, T. Vosch, A. Stesmans, B. Sels, S. De Gendt, *J. Phys. Chem. C* **2010**, *114*, 6894.

[53] W. J. Zhu, V. Perebeinos, M. Freitag, P. Avouris, *Phys. Rev. B* **2009**, 80.
[54] H. C. Cheng, R. J. Shiue, C. C. Tsai, W. H. Wang, Y. T. Chen, *ACS Nano* **2011**, *5*, 2051.
[55] a) N. Stander, B. Huard, D. Goldhaber-Gordon, *Phys. Rev. Lett.* **2009**, *102*; b) A. F. Young, P. Kim, *Nat. Phys.* **2009**, *5*, 222–226.
[56] J. R. Williams, L. DiCarlo, C. M. Marcus, *Science* **2007**, *317*, 638.
[57] V. V. Cheianov, V. Fal'ko, B. L. Altshuler, *Science* **2007**, *315*, 1252.
[58] a) K. Brenner, R. Murali, *Appl. Phys. Lett.* **2010**, 96; b) T. Lohmann, K. von Klitzing, J. H. Smet, *Nano Lett.* **2009**, *9*, 1973; c) E. C. Peters, E. J. H. Lee, M. Burghard, K. Kern, *Appl. Phys. Lett.* **2010**, 97.